

## *Undeformed Chip Shape in Angular Grinding*

Toshikatsu NAKAJIMA\* and Heisaburo NAKAGAWA\*

(Received June, 6, 1975)

### Synopsis

This paper describes the basic boundary conditions in angular grinding, which is widely applied as a high efficiency machining and where a complicated-shaped workpiece is ground at the same time.

The angular grinding is first classified into three basic types, an external, a surface and an internal angular grinding, depending on the axis angle between the wheel and the work axes.

The undeformed chip shape, which is characterized by the interference angle, the maximum chip thickness and the chip length, is then analyzed in each type of angular grinding.

The effects of grinding conditions such as the axis angle, the speed ratio, the radius ratio and the successive cutting edge spacing upon the geometry of undeformed chip are discussed to make clear the relations between the basic boundary conditions and the working conditions in angular grinding.

### 1. Introduction

All machining processes aim at the increase of added-values such as accuracy and quality to machined parts at great productivity and low cost. An ideal machining process is then one in which the oper-

---

\* Department of Mechanical Engineering

ating conditions yield high efficiency, higher accuracy, better surface integrity and lower cost.

Therefore an ideal machining process implies free cutting at high cutting speed and small cutting depth with multi-cutting edge tool. In other words, a small cutting depth is indispensable to high accuracy and good surface integrity and on the other hand results in low machining efficiency if single point tool is used in a process. The machining efficiency can however be improved by adopting high cutting speed and multi-cutting edged tool. Thus, a machining process at high cutting speed and small cutting depth with multi-cutting edged tool yields high efficiency, high accuracy, good surface integrity and low cost.

The grinding process is operated at the highest cutting speed and the smallest cutting depth with the greatest number of cutting edges of all machining processes. The grinding process can therefore be the most ideal one and has widely been applied as high efficiency and high accuracy machining.

The grinding efficiency is affected by relative grinding speed, cutting depth of wheel and wheel width, and is significantly improved with increasing any of these working conditions. The high speed grinding, which is developed recently and adopted widely, is one in which the grinding efficiency is drastically improved by increasing relative grinding speed, and in the heavy grinding the high grinding efficiency can be obtained by increasing cutting depth of wheel. Furthermore, the angular form grinding, which is recently marked as a high efficiency machining, is one in which a wide grinding wheel is used to grind a complicated-shaped workpiece at the same time and the wide grinding wheel is plunged at a certain angle to the center axis of workpiece. In the angular form grinding the complicated profile on the wide grinding wheel makes a great difference in the interference conditions between wheel and workpiece on each section in the wheel axis direction, and then the coarser roughness, the grinding burn and the grinding crack in the extreme are found partly on the ground surface.

In this paper, the angular grinding is first classified into three basic types of grinding depending on the axis angle between the wheel and the work axes. The undeformed chip shape, which is characterized by the interference angle, the maximum chip thickness and the chip length, is then analyzed in each type of angular grinding. Effects of grinding conditions such as the axis angle, the speed ratio, the radius ratio and the successive cutting edge spacing upon the geometry of undeformed chip are discussed to make clear the relations between the

basic boundary conditions and the working conditions in angular grinding.

2. Classification of Angular Grinding

In the angular form grinding the complicated-shaped workpiece is ground at the same time with the wide grinding wheel, which has the same profile as in the workpiece and is plunged at a certain angle to the work center axis, as shown in Fig.1. Denoting the axis angle between wheel and work axes, the wheel surface angle between wheel surface and wheel axis, and the work surface angle between work surface and work axis by  $\phi$ ,  $\theta_s$  and  $\theta_w$  in Fig.1, the following relation is found between these angles,

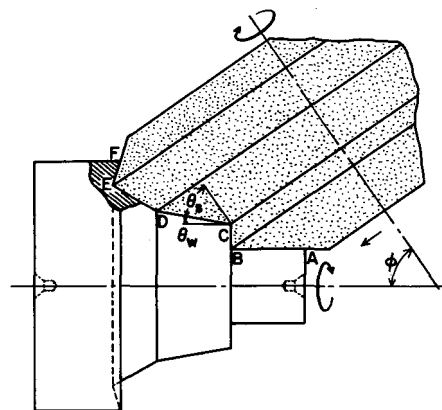


Fig. 1 Angular Form Grinding

$$\phi = \theta_s + \theta_w \quad (1)$$

The interference conditions between wheel and workpiece are then affected by two angles of the axis, the wheel surface and the work surface angle in the angular form grinding. In other words, the axis angle  $\phi$  or the wheel surface angle  $\theta_s$  can freely be selected in the angular form grinding of the workpiece that has the designed profile and then the designed work surface angle  $\theta_w$ . In this case the interference conditions between wheel and workpiece can be analyzed in several simple-shaped segments which are characterized by the angles. For example, the grinding width is divided into five segments in the angular form grinding in Fig.1 and the characteristic angles on each segment, by which the interference conditions are characterized, are shown in Table 1. Furthermore as seen in Fig.1, the axis angle  $\phi$

Table 1. Characteristic Angles in Angular Form Grinding shown in Fig.1

Segments	$\theta_w$ (deg.)	$\theta_s$ (deg.)	$\phi = \theta_s + \theta_w$ (deg.)
AB	0	55	55
BC	90	-35	
CD	10	45	
DE	30	25	
EF	105	-50	

and the work surface angle  $\theta_w$  can be selected within the ranges in the following,

$$0 \leq \phi \leq \pi, \quad 0 \leq \theta_s \leq \pi \quad (2)$$

As mentioned above, the angular form grinding of a complicated-shaped workpiece is composed of the angular grinding of several simple-shaped workpieces.

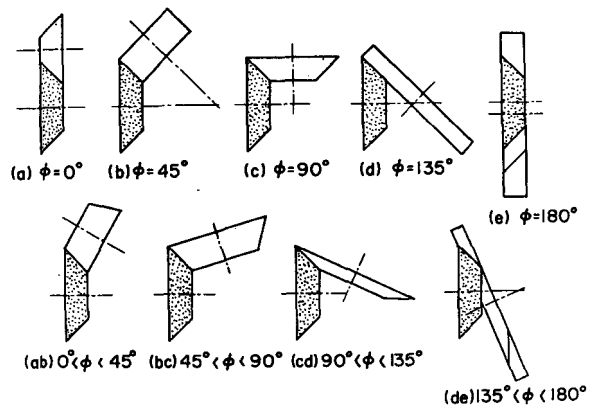


Fig.2 shows some possible types of angular grinding on varying the axis angle  $\phi$  within the range in Eq.(2) for  $\theta_s = 45^\circ$ . As seen in the figure, the angular grinding for  $0 \leq \phi < 90^\circ$  corresponds to the external one, because any section of wheel perpendicular to the wheel axis exists in the different domain from the one where the projected section of workpiece on a plane perpendicular to the wheel axis does. The angular grinding for  $\phi = 90^\circ$  corresponds to the surface one, because the moving plane of abrasive grains is perpendicular to the moving plane of workpiece. Furthermore, the angular grinding for  $90^\circ < \phi \leq 180^\circ$  corresponds to the internal one, because any section of wheel perpendicular to the wheel axis exists in the same domain as the one where the projected section of workpiece on a plane perpendicular to the wheel axis does. As mentioned above, three basic types of grinding, the external, the surface and the internal grinding, appear in the angular grinding, depending on the axis angle between wheel and work axes.

### 3. Analysis of Undeformed Chip Shape in Angular Grinding

All the mechanical machining operations utilize the chip formation process where the relative motion and position between the tool and workpiece produce the chip. Practical development of machining cannot, therefore, be made until the chip formation physics is clearly understood. This is clear from the fact that the two-dimensional cutting theory has played a great role in the analysis of the cutting mechanism for a single cutting edge such as in turning and aided significantly in the development.

Most investigations on conventional grinding to the present time has been conducted based on the basic boundary conditions which can be made

clear by analyzing undeformed chip shape in conventional grinding. This approach has been significantly useful in developing conventional grinding process, and has made it clear that the cutting process in grinding is transitional and then the accumulation phenomenon due to the transitional cutting affects grinding process[1-6].

Therefore in order to understand fundamentally and improve significantly the angular grinding process, the undeformed chip shape should first be analyzed to make clear the basic boundary conditions in the angular grinding and to discuss the relations between the basic boundary conditions and the working conditions.

From the above point of view, the undeformed chip shape in the angular grinding, which is characterized by the interference angle, the maximum chip thickness and the chip length, is theoretically analyzed to make clear effects of the working conditions such as the axis angle, the speed ratio, the radius ratio and the successive cutting edge spacing upon the geometry of undeformed chip.

Fig.3 shows a schematic model of the angular grinding. As seen in the figure, the parameters, which should be taken into consideration on analyzing undeformed chip shape in the angular grinding, increase in number as compared with in conventional grinding.

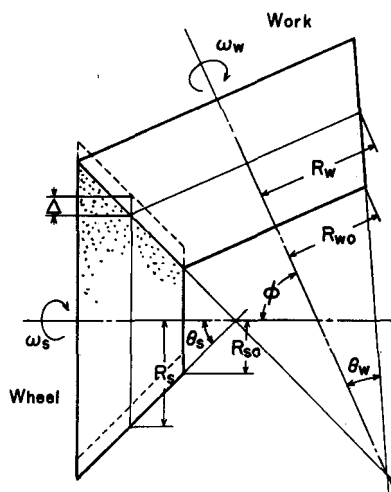


Fig. 3 Schematic Model of Angular Grinding

### 3.1 The Locus of a Cutting Edge on the Workpiece Surface.

The locus of a cutting edge of the wheel relative to the workpiece is a fundamental curve on the analysis of undeformed chip shape in grinding. The general equation of theoretical interference curve between a cutting edge and workpiece should therefore be obtained to analyze the interference angle, the maximum chip thickness and the chip length which characterize the geometry of undeformed chip in the angular grinding.

Fig.4 shows the interference between wheel and workpiece in a section of the angular grinding in Fig.3, which is projected on a plane perpendicular to the wheel axis. In this case, the profile of the imagining section of workpiece is projected as an ellipse with the major radius  $R_w$  and the minor radius  $R_w \cos \phi$  because of the axis angle  $\phi$  between the wheel and the work axes, while that of wheel is done as a

circle. Therefore, a point on the work surface, which moves at a uniform speed  $V_w$  on the circle, moves at an irregular speed on the ellipse on the projection plane. The peripheral speed of workpiece at the point M on the ellipse is however equal to the actual peripheral speed of workpiece  $V_w$ .

Since the setting depth of wheel  $\Delta$  is normally small and then the arc of contact between the wheel and work is very small, the ellipse representing the profile of the work section can be replaced by the equivalent circle of the radius  $R'_w$ , which revolves at a uniform angular velocity  $\omega'_w$ , on analyzing the locus of a cutting edge relative to the workpiece. In this case the curvature of the equivalent circle should be equal to that of the ellipse at the point M. The radius  $R'_w$  of the equivalent circle is then given by the equation,

$$R'_w = R_w / \cos\phi \quad (3)$$

On the other hand, the peripheral speed of a point on the equivalent circle should be equal to that on the ellipse at the point M. From this condition the angular velocity  $\omega'_w$  of the equivalent circle can be given by the equation,

$$\omega'_w = V_w / R'_w = \omega_s \cdot \cos\phi \quad (4)$$

Now, the travelling of a cutting edge I of the wheel on the workpiece is observed in Fig.4. The cutting edge I contacts the workpiece during the angle  $2\alpha_s$  around the center of the wheel and then the travelling time T of the cutting edge I on the workpiece can be given in the form,

$$T = 2\alpha_s / \omega_s \quad (5)$$

where  $\omega_s$  is the angular velocity of the grinding wheel.

While the grinding wheel rotates on the center by the angle  $2\alpha_s$  and the cutting edge I contacts the workpiece by the angle  $(2\alpha'_w + \beta')$  around the center of workpiece, the workpiece does by the angle  $\beta'$  on the center

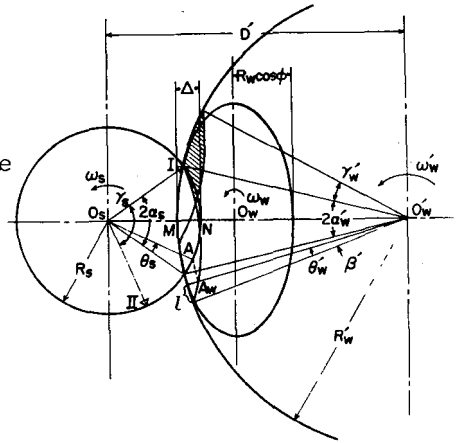


Fig. 4 Interference between Wheel and Workpiece in Angular Grinding

of workpiece. Then

$$\beta' = \omega'_w \cdot T = 2\alpha'_s \cdot K'_\omega \quad (6)$$

$$\text{where } K'_\omega = \omega'_w / \omega'_s.$$

The point A where the cutting edge I cuts the workpiece on the rotation of wheel by the angle  $\theta'_s$  corresponds to the point  $A'_w$  on the interference curve and the radius of  $\theta'_w$  in angle around the work center, joining the work center and the point of l in arc length from the beginning point of contact between the cutting edge I and the workpiece surface. Then,

$$\theta'_w = \frac{l}{R'_w} = \frac{2\alpha'_w + \beta'}{2\alpha'_s} \cdot \theta'_s = (K'_\alpha + K'_\omega) \theta'_s \quad (7)$$

$$\theta'_s = \frac{l}{R'_w} \cdot \frac{1}{K'_\alpha + K'_\omega}$$

$$\text{where } K'_\alpha = \alpha'_w / \alpha'_s.$$

The interference depth  $t_\theta$  of the cutting edge I in the radial direction at the point  $A'_w$  is, as easily checked in the triangle  $O'_s O'_w A$  in Fig.4, given by the equation,

$$\begin{aligned} t_\theta &= R'_w - \overline{O'_w A} \\ &= R'_w - \sqrt{D'^2 + R_s^2 - 2D'R_s \cos(\alpha'_s - \theta'_s)} \\ &= \Delta - \frac{R_s + R'_w}{2K'_R} (\alpha'_s - K'_1 \cdot l)^2 \end{aligned} \quad (8)$$

where  $\Delta$  is the setting depth of wheel,  $K'_R = R'_w / R_s$ ,  
and  $K'_1 = l/R'_w (K'_\alpha + K'_\omega) = l/R_s (1 + K'_V)$ .

On the other hand, the angle  $2\alpha'_s$  around the wheel center during which the cutting edge I contacts the workpiece can be given as (see Fig.4)

$$\alpha'_s = \sqrt{\frac{K'_R}{1 + K'_R} \cdot \frac{2\Delta}{R_s}} \quad (9)$$

The distance L on the workpiece surface between the beginning point and the end of contact of the cutting edge I is given by the equation,

$$L = R'_w (2\alpha'_w + \beta') \doteq 2\alpha'_w R'_w \left( 1 + \frac{K'_V}{K'_R + K'_\alpha} \right) \quad (10)$$

$$\text{where } K'_V = V_w / V_s = K'_R \cdot K'_\omega.$$

### 3.2 Chip Thickness and Chip Length.

It is well known that the cutting depth of tool in turning is an important value on analyzing the cutting efficiency, the accuracy, the roughness of the turned surface and so on. The equivalent in grinding for the cutting depth of tool in turning is not the setting depth of wheel, but the cutting depth of each grain. The cutting depth of a grain has a direct effect upon the grinding force, the grinding temperature, the depth of affected layer, the wheel wear, the surface roughness and so on. The cutting depth of a grain is therefore a fundamental value on analyzing the grinding process.

From this point of view, general equations for the cutting depth of a grain and the chip length are obtained in the most available form on analyzing various phenomena in grinding, based upon the interference curve obtained previously.

In practical grinding operations, the cutting edge II successive to the cutting edge I cuts the workpiece and the geometrical form of undeformed chip is as the shadowed portion in Fig.4.

Denoting the successive cutting edge spacing by  $\delta$  and putting

$$\gamma_s = \delta / R_s, \quad \gamma'_w = K'_w \cdot \gamma_s = K'_w \delta / R_s$$

the distance  $L_0$  on the workpiece surface between the the ends of cut of the cutting edges I and II can be given in the form

$$L_0 = R'_w \cdot \gamma'_w = K'_w \cdot K'_R \cdot \delta = K_V \cdot \delta \quad (11)$$

From Eq.(8) and (11), the general equations  $t_{\theta I}$  and  $t_{\theta II}$  of interference curves of the cutting edges I and II, which are function of the distance  $l$  from the end of cut, are in the forms,

$$\left. \begin{aligned} t_{\theta I} &= \Delta - \frac{R_s + R'_w}{2K'_R} (\alpha_s - K_1 \cdot l)^2 \\ t_{\theta II} &= \Delta - \frac{R_s + R'_w}{2K'_R} \{ \alpha_s - K_1 \cdot (l - L_0) \} \end{aligned} \right\} (12)$$

As indicated in Fig.5, the undeformed chip shapes are classified into three basic types as follows:

Type I : The maximum chip thickness  $t_{\max}$  is always smaller than the cutting depth of wheel  $\Delta$ .

$$t_{\max} < \Delta, L_o < L/2$$

Type II : The maximum value is equal to the cutting depth of wheel  $\Delta$ .

$$t_{\max} = \Delta, L/2 \leq L_o \leq L$$

Type III : There are parts of the work surface which are not cut.

$$t_{\max} = \Delta, L < L_o$$

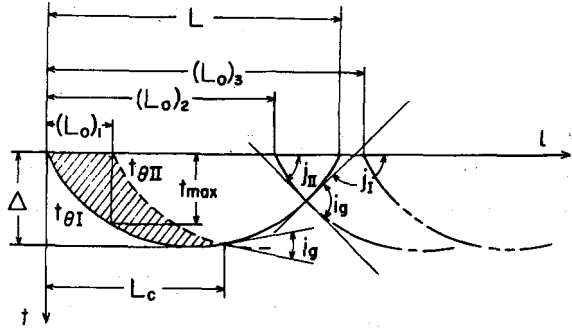


Fig. 5 Undeformed Chip Shape

It is desirable that chip types I and II are used during grinding. For chip types I and II the chip thickness  $t$  can be obtained as follows:

$$t = t_{\theta} = \Delta - \frac{R_s + R'_w}{2K'_R} (\alpha_s - K_1 \cdot l)^2, (0 \leq l \leq L_o) \quad (13)$$

$$t = t_{\theta I} - t_{\theta II} = \frac{R_s + R'_w}{2K'_R} \cdot K_1 \cdot L_o (2\alpha_s + K_1 L_o - 2K_1 \cdot l), (L_o \leq l \leq L_c) \quad (14)$$

where  $L_c$  is the chip length.

The maximum chip thickness  $t_{\max}$  is equal to the cutting depth of wheel  $\Delta$  for chip types II and III, as seen in Fig.5. For chip type I the chip thickness becomes maximum in  $l=L_o$  and then the maximum chip thickness  $t_{\max}$  can be obtained as follows (see Fig.5):

$$t_{\max} = \frac{R_s + R'_w}{2K'_R} K_1 \cdot L_o (2\alpha_s - K_1 \cdot L_o) \quad (15)$$

The chip length  $L_c$  for chip types I and II can be given by the value of  $l$  at the point of intersection of the interference curves of the successive cutting edges. Then, from Eq.(12),

$$L_c = \frac{\alpha_s}{K_1} + \frac{L_o}{2} = \alpha_s R_s (1 + K_V) + \frac{L_o}{2} \quad (16)$$

For chip type III the chip length  $L_c$  is equal to the length  $L$  on the work surface between the beginning and the end of contact of a grain with workpiece. From Eq.(10),

$$L_c = L = R'_w ( 2\alpha'_w + \beta' ) = 2\alpha_s R_s ( 1 + K_V ) \quad (17)$$

In the analysis of the geometry of the undeformed chip shape, the equivalent work radius  $R'_w$  has been used for the actual work radius  $R_w$ . Using the relation in Eq.(3), the final expressions for the maximum chip thickness and the chip length in angular grinding are as follows:

$$t_{\max} = \frac{1}{2} \cdot \frac{K_R + \cos\phi}{K_R} \cdot \frac{K_V}{(1+K_V)^2} \cdot \frac{\delta}{R_s} [2\alpha_s R_s (1+K_V) - L_o] \quad (18)$$

$$L_c = \alpha_s R_s (1+K_V) + \frac{L_o}{2} \quad (19)$$

where

$$\alpha_s = \sqrt{\frac{K_R}{K_R + \cos\phi} \cdot \frac{2\Delta}{R_s}} \quad (20)$$

### 3.3 Interference Angle.

In grinding the cutting depth of a grain is very small and the cutting edge contacts the workpiece at a very small angle. These two conditions are quite different than those encountered in turning. The grinding process involves three distinct regions. First, the metal being cut is only elastically deformed from the contact with the cutting edge, then plastically deformed and finally cut with an increase in the cutting depth.

The first region where the cutting edge slides on the surface of the workpiece without cutting is very important because this length of sliding has a direct affect upon stock removal, wear of the cutting edge, grinding temperature, and an indirect effect upon the pile-up phenomena, accuracy, roughness and the surface layer. Therefore, the various phenomena at the beginning of contact must be understood before the chip formation physics of grinding can be clearly explained.

One of the most important concepts introduced to clear up this point is the interference angle  $i_g$ . This is important because the critical cutting depths(maximum elastic and plastic deformations) are constants of the material for a given contact area in clearance surface of a cutting edge and cutting velocity and, therefore, the sliding length and the plastic length will increase with a decrease in the interference angle  $i_g$ . From the above mentioned point of view, the interference

angle  $i_g$  important to describe many grinding phenomena are analyzed.

Denote the angles at which the tangents of interference curves of successive cutting edges in  $l=L_c$  intersect the  $l$ -axis in Fig.5 by  $j_I$  and  $j_{II}$ , respectively. Then, from Eq.(12),

$$\left. \begin{aligned} \tan j_I &= \frac{K_1}{K'_R} (R_s + R'_w) (\alpha_s - K_1 \cdot L_c) \\ \tan j_{II} &= \frac{K_1}{K'_R} (R_s + R'_w) [\alpha_s - K_1 (L_c - L_o)] \end{aligned} \right\} (21)$$

On the other hand the interference angle  $i_g$  can be given by  $j_I$  and  $j_{II}$  in the equation,

$$\tan i_g = \tan(j_{II} + \pi - j_I) \quad (22)$$

Substituting Eq.(21) into Eq.(22) and putting  $\tan i_g \doteq i_g$  because the interference angle  $i_g$  is in general very small,

$$i_g = \frac{1+K'_R}{K_R} \cdot \frac{K_V}{(1+K_V)^2} \cdot \frac{\delta}{R_s} \quad (23)$$

Using the relation in Eq.(3) the interference angle  $i_g$  in angular grinding is given in the form,

$$i_g = \frac{K_R + \cos\phi}{K_R} \cdot \frac{K_V}{(1+K_V)^2} \cdot \frac{\delta}{R_s} \quad (24)$$

#### 4. Typical Theoretical Results

In the previous section the fundamental and important equations concerning the wheel-work conformity in angular grinding have been developed. In this section typical trends predicted by these equations will be illustrated and the implications of these trends indicated.

As mentioned previously the angular grinding is characterized by the axis angle  $\phi$  between the wheel and the work axes. In other words, the angular grinding falls into cylindrical for  $0 \leq \phi < 90^\circ$ , the surface for  $\phi = 90^\circ$  and the internal grinding for  $90^\circ < \phi \leq 180^\circ$ , respectively.

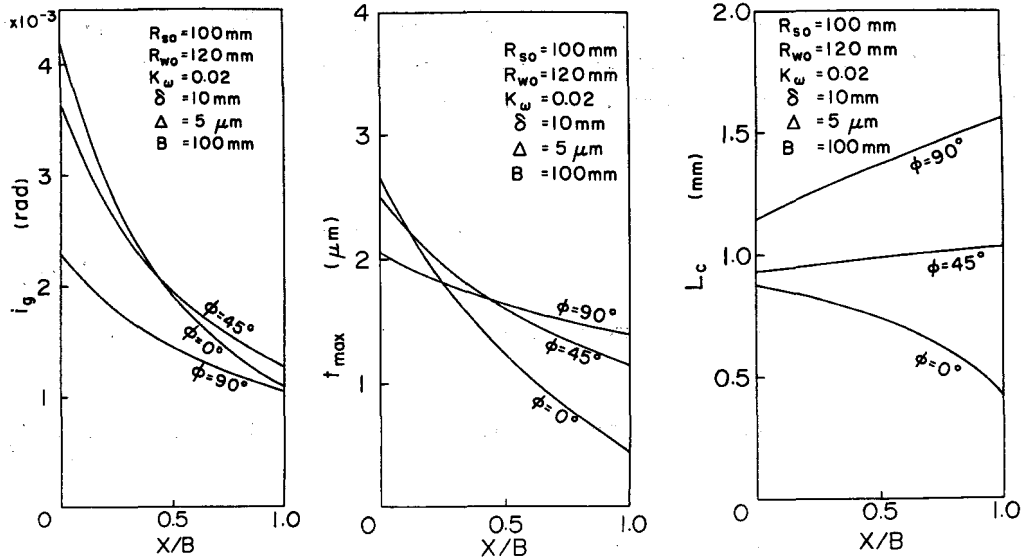


Fig. 6 Characteristic Values of Undeformed Chip in External and Surface angular Grinding

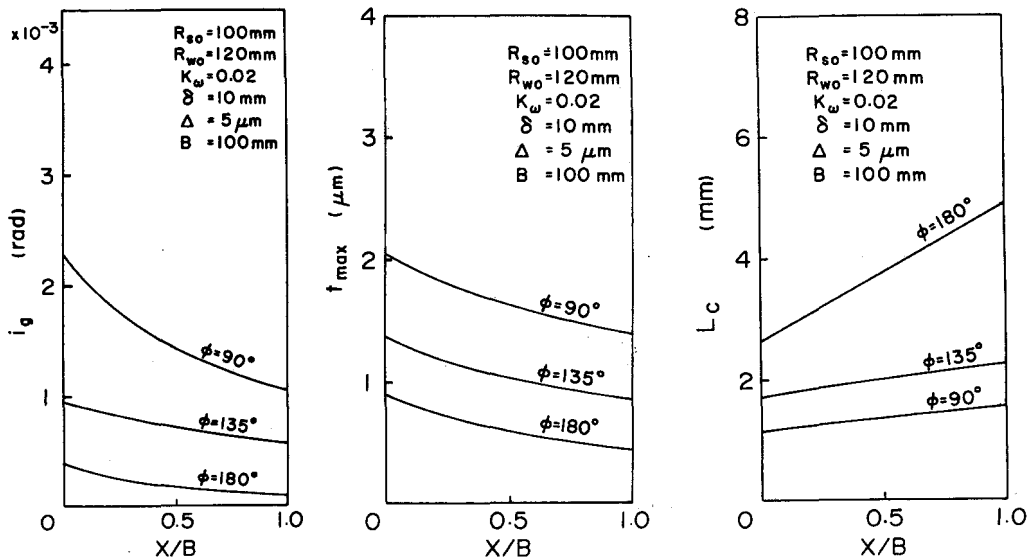


Fig. 7 Characteristic Values of Undeformed Chip in Surface and Internal Angular Grinding

Fig.6 and Fig.7 show variations of the interference angle, the maximum chip thickness and chip length with the distance  $X$  in the wheel axis direction from the wheel face of the smallest sectional area for the external, the surface and the internal angular grinding (cf. Fig.3 ). As can be easily seen in the figures, the interference angle and the

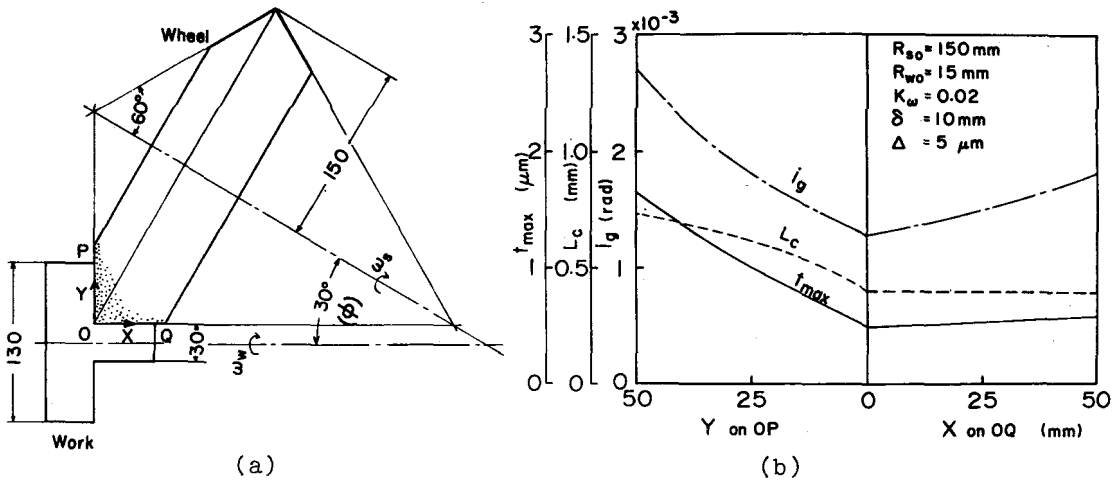


Fig. 8 Undeformed Chip Shape in Angular Form Grinding

maximum chip thickness decrease with an increase of the distance from the smallest sectional area wheel face for any type of the angular grinding and then the chip length increases with increasing the distance except for  $\phi=0^\circ$ .

Fig.8(a) shows an example of the angular grinding of the shaft with a flange where a face of the flange and a peripheral surface of the shaft are ground at the same time. In such an angular grinding the detriment of surface integrity is often observed on the inner part of the face, though the grinding is external both on the face and the peripheral surface. Fig.8(b) shows the distributions of the interference angle, the maximum chip thickness and the chip length on the surface OP and on the peripheral surface OQ. As seen in the figure, any of the interference angle, the maximum chip thickness and the chip length increases with increasing the distance from the

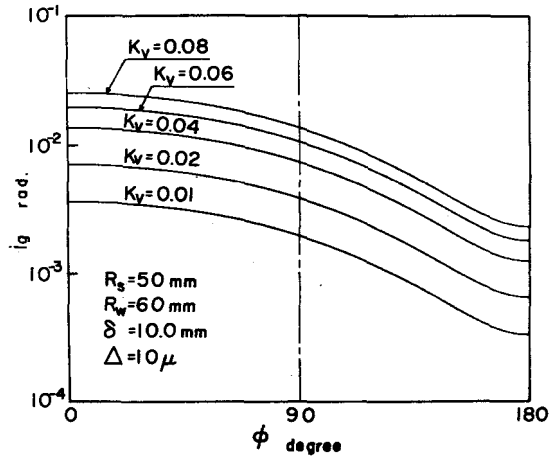


Fig. 9 Effects of Speed Ratio on Interference Angle

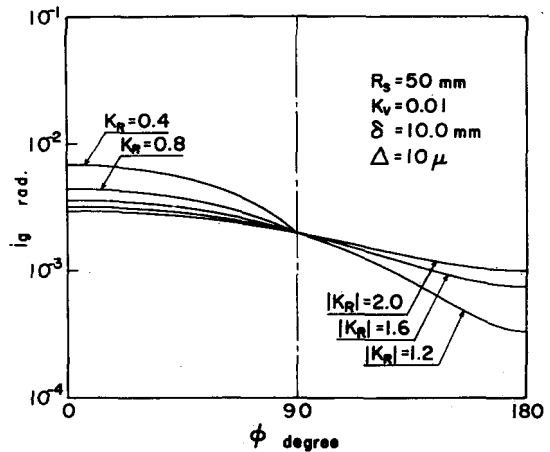


Fig. 10 Effects of Radius Ratio on Interference Angle

point O and therefore the undeformed chip shape on the face is larger than that on the peripheral surface. This indicates that the larger grinding energy is necessary on the face as compared with on the peripheral surface and then the detriment of surface integrity can be observed on the face.

Fig.9, Fig.10 and Fig.11 show effects of grinding conditions such as the axis angle  $\phi$ , the speed ratio  $K_V$ , the radius ratio  $K_R$  and the successive cutting edge spacing  $\delta$ , upon the interference angle. As seen in these figures, the interference angle increases with decreasing the axis angle and with increasing the speed ratio and the successive cutting edge spacing, and then the interference angle increases with decreasing the radius ratio for the external angular grinding and with increasing the radius ratio for the internal one.

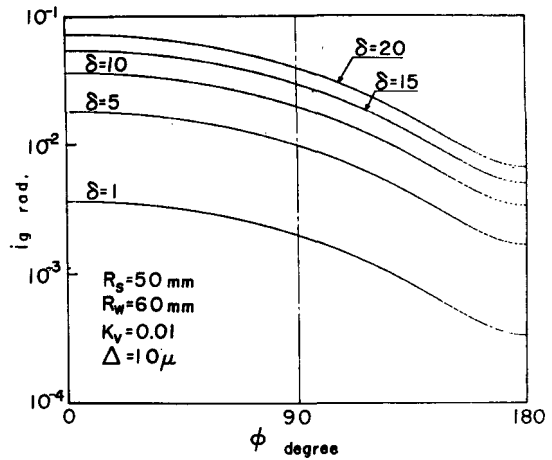


Fig. 11 Effects of Successive Cutting Edge Spacing on Interference Angle

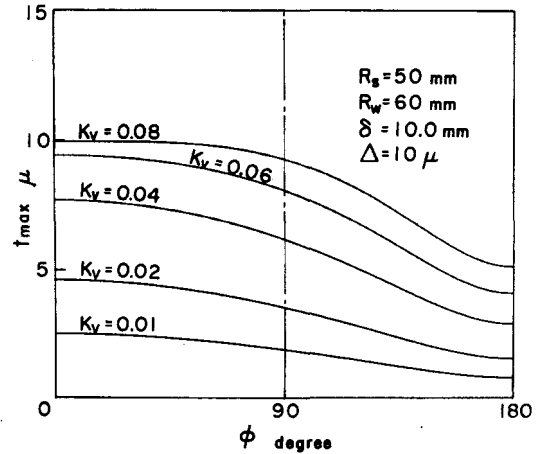


Fig. 12 Effects of Speed Ratio on Maximum Chip Thickness

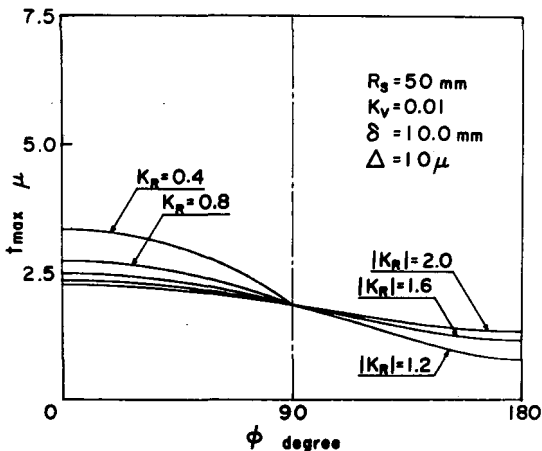


Fig. 13 Effects of Radius Ratio on Maximum Chip Thickness

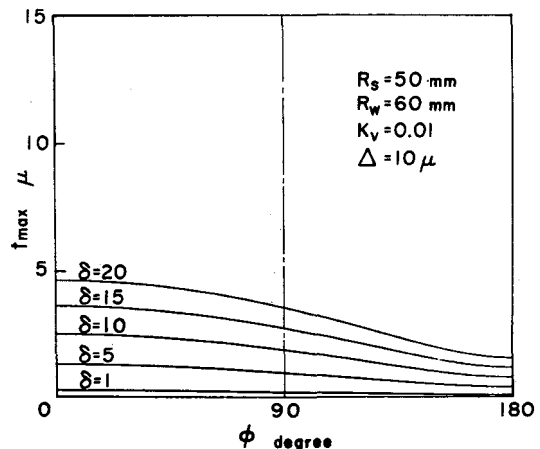


Fig. 14 Effects of Successive Cutting Edge Spacing on Maximum Chip thickness

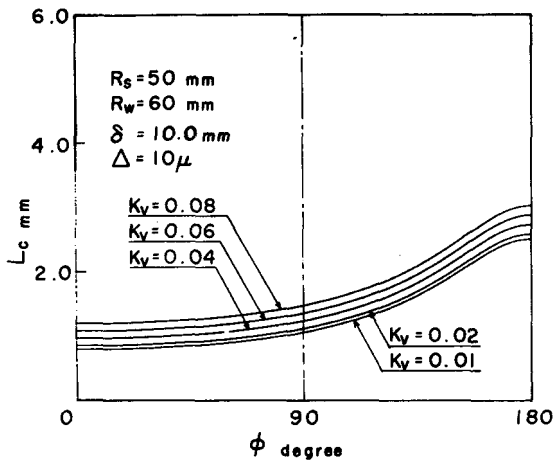


Fig. 15 Effects of Speed Ratio on Chip Length.

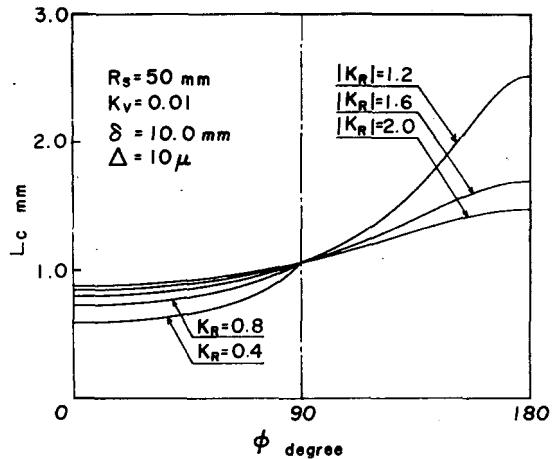


Fig. 16 Effects of Radius Ratio on Chip Length

Fig.12, Fig.13 and Fig.14 show effects of the grinding conditions such as mentioned previously upon the maximum chip thickness. Note in these figures that effects of the grinding conditions upon the maximum chip thickness are the same as those upon the interference angle.

Fig.15, Fig.16 and Fig.17 show also effects of the grinding conditions such as mentioned previously upon the chip length. It should be noted that the chip length becomes larger with increasing the axis angle, the speed ratio and the successive cutting edge spacing, and that the chip length increases with increasing the radius ratio for the external angular grinding and with decreasing the radius ratio for the internal one.

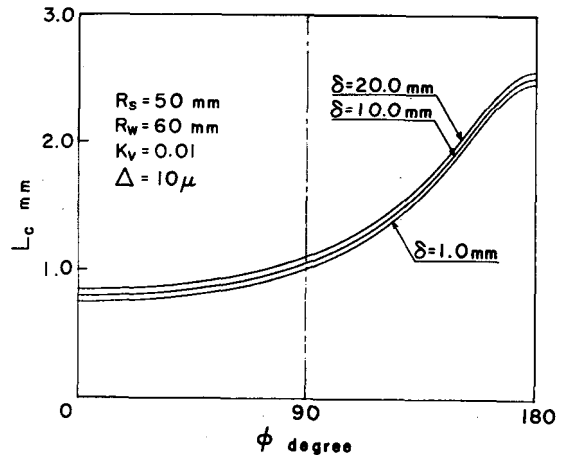


Fig. 17 Effects of Successive Cutting Edge Spacing on Chip Length

## 5. Conclusions

Scientific understanding and practical development of angular grinding cannot be made until the basic boundary conditions are made

clear. From this point of view, the undeformed chip shape in angular grinding, which is characterized by interference angle, the maximum chip thickness and the chip length, has been analyzed and it has been discussed how the geometry of undeformed chip is affected by working conditions such as the axis angle, the speed ratio, the radius ratio and the successive cutting edge spacing.

#### References

- (1) K. Okamura and T. Nakajima : Analysis of Transitional Cutting Process, Trans. S.M.E., vol. 1 ( 1972 ) 55
- (2) K. Okamura and T. Nakajima : Study of Cutting Mechanism of Abrasive Grain ( 5th Report ), Journal of J.S.P.E., vol.33, No. 4 ( 1967 ) 237
- (3) K. Okamura and T. Nakajima : Fundamental Analysis of Grinding Process, S.M.E. Technical Paper, MR70-183 ( 1970 )
- (4) K. Okamura and T. Nakajima : The Surface Generation Mechanism in the Transitional Cutting Process, Proc. of the International Grinding Conference, Pittsburgh, Pa., ( 1972 ) 306
- (5) K. Okamura and T. Nakajima : Size Generation Process in Grinding, Proc. of the International Conference on Production Engineering, ( 1974 ) 62
- (6) T. Nakajima and K. Okamura : Transient Characteristic in Grinding ( 3rd Report ), Journal of J.S.P.E., vol.40, No. 3 (1974) 256